

A Variational Approach to Privacy and Fairness

Borja Rodríguez-Gálvez, Ragnar Thobaben, and Mikael Skoglund

Division of Information Science and Engineering (ISE)

KTH Royal Institute of Technology

{borjarg, ragnart, skoglund}@kth.se

Abstract

In this article, we propose a new variational approach to learn private and/or fair representations. This approach is based on the Lagrangians of a new formulation of the privacy and fairness optimization problems that we propose. In this formulation, we aim at generating representations of the data that keep a prescribed level of the relevant information that is not shared by the private or sensitive data, while minimizing the remaining information they keep. The proposed approach (i) exhibits the similarities of the privacy and fairness problems, (ii) allows us to control the trade-off between utility and privacy or fairness through the Lagrange multiplier parameter, and (iii) can be comfortably incorporated to common representation learning algorithms such as the VAE, the β -VAE, the VIB, or the nonlinear IB.

1 Introduction

Currently, many systems rely on machine learning algorithms to make decisions and draw inferences. That is, they use previously existing data in order to shape some stage of their decision or inference mechanism. Usually, this data contains private or sensitive information, e.g., the identity of the person from which a datum was collected or their membership to a minority group. Therefore, an important problem occurs when the data used to train such algorithms leaks this information to the system, thus contributing to unfair decisions or to a privacy breach.

When the content of the private or sensitive information is arbitrary and the task of the system is not defined, the problem is reduced to learning *private representations* of the data; i.e., representations that are informative of the data (utility), but are not informative of the private or sensitive information. Then, these representations can be employed by any system with a controlled leakage of private information. If the level of informativeness is measured with the mutual information, the problem of generating private representations is known as the *privacy funnel* (PF) (du Pin Calmon and Fawaz 2012; Makhdomi et al. 2014).

When the task of the system is known, then the aim is to design strategies so that the system performs such a task efficiently while obtaining or leaking little information about the sensitive data. The field of *algorithmic fairness*

has extensively studied this problem, especially for classification tasks and categorical sensitive data; see, e.g., (Dwork et al. 2012; Zafar et al. 2017; Chouldechova and Roth 2018; Corbett-Davies and Goel 2018). An interesting approach is that of learning *fair representations* (Zemel et al. 2013; Edwards and Storkey 2016; Zhao et al. 2020), where similarly to their private counterparts, the representations are informative of the task output, but are not informative of the sensitive information.

There is a compromise between information leakage and utility when designing private representations (Makhdomi et al. 2014). Similarly, in the field of algorithmic fairness, it has been shown empirically (Calders, Kamiran, and Pechenizkiy 2009) and theoretically (Zhao and Gordon 2019) that there is a trade-off between fairness and utility.

In this work, we investigate the trade-off between utility and privacy and between utility and fairness in terms of mutual information (details about the choice of mutual information in Appendix F). More specifically, we aim at maintaining a certain level of the information about the data (for privacy) or the task output (for fairness) that is not shared by the sensitive data, while minimizing all the other information. We name these two optimization problems the *conditional privacy funnel* (CPF) and the *conditional fairness bottleneck* (CFB) due to their similarities with the privacy funnel (Makhdomi et al. 2014), the information bottleneck (IB) (Tishby, Pereira, and Bialek 2000), and the recent conditional entropy bottleneck (CEB) (Fischer 2020).

We tackle both optimization problems with a variational approach based on their Lagrangian. For the privacy problem, we show that the minimization of the Lagrangians of the CPF and the PF is equivalent (see Appendix A.2), meaning that our variational approach attempts at solving the PF as well. Moreover, this approach improves over current variational approaches to the PF by respecting the problem’s Markov chain in the encoder distribution.

Finally, the resulting approaches for privacy and fairness can be implemented with little modification to common algorithms for representation learning like the variational autoencoder (VAE) (Kingma and Welling 2013), the β -VAE (Higgins et al. 2017), the variational information bottleneck (VIB) (Nan and Tao 2020), or the nonlinear information bottleneck (Kolchinsky, Tracey, and Wolpert 2019). Therefore, it facilitates the incorporation of private and fair representa-

tions in current applications (see Appendix B for a guide on how to modify these algorithms).

We demonstrate our results both in the Adult dataset, available at the UCI repository (Dua and Graff 2017), which is commonly employed for benchmarking both tasks, and a high-dimensional toy dataset, based on the MNIST handwritten digits dataset (LeCun et al. 1998). Further experiments on the COMPAS dataset (Dieterich, Mendoza, and Brennan 2016) can be found in Appendix D.

2 Methods

In this section we give an overview of our approach. First, we introduce our proposed model for the privacy and fairness problems. Then, we present a suitable Lagrangian formulation. Finally, we describe a variational approach to solving both problems.

2.1 Problem formulation

Privacy formulation: the conditional privacy funnel (CPF) Let us consider two random variables $X \in \mathcal{X}$ and $S \in \mathcal{S}$ such that $I(X; S) > 0$. The random variable X represents some data we want to share, and the random variable S represents some private data. We wish to disclose the data of interest X ; however, we do not want the receiver of this data to draw inferences about the private data S . For this reason, we encode the data of interest X into the representation $Y \in \mathcal{Y}$, forming the Markov chain $S \leftrightarrow X \rightarrow Y$.

This encoding, characterized by the conditional probability distribution $P_{Y|X}$, is designed so that the representation Y keeps a certain level r of the information about the data of interest X that is not shared by the private data S (i.e., the light gray area in Figure 1a), while minimizing the information it keeps about the private data S (i.e., the dark gray area in Figure 1a). That is,

$$\arg \inf_{P_{Y|X}} \{I(S; Y)\} \text{ s.t. } I(X; Y|S) \geq r. \quad (1)$$

The main difference with the privacy funnel formulation (Makhdoumi et al. 2014) is that, even though both formulations minimize the information the representation Y keeps about the private data S , in the PF the encoding is designed so that Y keeps a certain level r' of the information about X , regardless if this information is also shared by S . Hence, even though the minimization of the Lagrangians of both problems is equivalent, the Lagrangian optimization of the CPF does not allow representations Y of X that filter private information arbitrarily (see Appendix A.2).

Fairness formulation: the conditional fairness bottleneck (CFB) Let us consider three random variables $X \in \mathcal{X}$, $S \in \mathcal{S}$, and $T \in \mathcal{T}$ such that $I(X; S) > 0$ and $I(S; T) > 0$. The random variable X represents some data we want to use to draw inferences about the task T . However, we do not want our inferences to be influenced by the sensitive data S . For this reason, we first encode the data X into a representation $Y \in \mathcal{Y}$, which is then used to draw inferences about T . Therefore, the Markov chains $S \leftrightarrow X \rightarrow Y$ and $T \leftrightarrow X \rightarrow Y$ hold.

This encoding, characterized by the conditional probability distribution $P_{Y|X}$, is designed so that the representation

Y keeps a certain level r of the information about the task output T that is not shared by the private data S (i.e., the light gray area in Figure 1b), while minimizing both the information it keeps about the private data S and the information about X that is not shared with the task output T (i.e., the dark and darker gray areas in Figure 1b, respectively). That is,

$$\arg \inf_{P_{Y|X}} \{I(S; Y) + I(X; Y|S, T)\} \text{ s.t. } I(T; Y|S) \geq r. \quad (2)$$

This formulation differs from other approaches to fairness mainly in two points: (i) Similarly to the IB (Tishby, Pereira, and Bialek 2000), the CFB does not only minimize the information the representations Y keep about the sensitive data S , but also minimizes the information about X that is not relevant to draw inferences about T . That is, the CFB seeks representations that are both *fair* and *relevant*, thus avoiding the risk of keeping *nuisances* (Achille and Soatto 2018) and harming their generalization capability. (ii) Similarly to the CEB (Fischer 2020), the CFB aims to produce representations Y that keep a certain level r of the information about the task T that is not shared by S . This differs from formulations that aim at producing representations that maintain a certain level r' of the information about T , regardless if it is also shared by the sensitive data S .

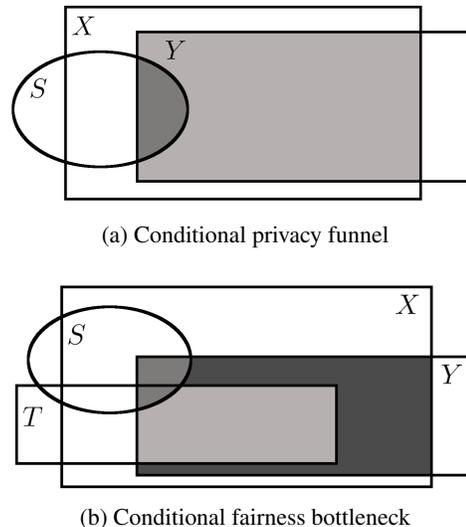


Figure 1: Information Diagrams (Yeung 1991) of (a) the conditional privacy funnel and (b) the conditional fairness bottleneck. In light gray, the relevant information we would like Y to keep. In dark and darker gray, the sensitive and irrelevant information, respectively, we would like Y to discard.

2.2 The Lagrangians of the problems

A common approach to solving optimization problems such as the CPF or the CFB is to minimize the *Lagrangian* of the problem. The Lagrangian is a proxy of the trade-off between the function to optimize and the constraints on the optimization search space (Boyd, Boyd, and Vandenberghe

where E is a random variable and $Y = f(X, E; \theta)$ is a deterministic function. Lastly, we estimate $p_{(S, X)}$ and $p_{(S, T, X)}$ as the data’s empirical densities.

In practice, if we have a dataset $D = \{(x^{(i)}, s^{(i)})\}_{i=1}^N$ for the CPF or $D = \{(x^{(i)}, s^{(i)}, t^{(i)})\}_{i=1}^N$ for the CFB, we minimize, respectively, the following cost functions:

$$\begin{aligned} \tilde{\mathcal{J}}_{\text{CPF}}(\theta, \phi, \gamma) &= \frac{1}{N} \sum_{i=1}^N D_{\text{KL}}(p_{Y|X=X^{(i)}, \theta} || q_{Y|\theta}) \\ &\quad - \gamma \mathbb{E}_{p_E} \left[\log \left(q_{X|(S=s^{(i)}, Y=f(x^{(i)}, E), \phi)}(x^{(i)}) \right) \right] \end{aligned} \quad (10)$$

$$\begin{aligned} \tilde{\mathcal{J}}_{\text{CFB}}(\theta, \phi, \beta) &= \frac{1}{N} \sum_{i=1}^N D_{\text{KL}}(p_{Y|X=X^{(i)}, \theta} || q_{Y|\theta}) \\ &\quad - \beta \mathbb{E}_{p_E} \left[\log \left(q_{T|(S=s^{(i)}, Y=f(x^{(i)}, E), \phi)}(t^{(i)}) \right) \right], \end{aligned} \quad (11)$$

where the expectation over $E \in \mathcal{E}$ is usually estimated with a naive Monte Carlo of a single sample; i.e., the expectation of $g(E) : \mathcal{E} \mapsto \mathbb{R}$ is estimated as $\mathbb{E}_{p_E}[g(E)] \approx \frac{1}{L} \sum_{l=1}^L g(\epsilon^{(l)})$, where $\epsilon^{(l)} \sim p_E$ and $L = 1$.

An *a posteriori* interpretation of this approach is that if the encoder compresses the representations Y assuming that the decoder will use both Y and the private or sensitive data S , then the encoder will discard the information about S contained in the original data X in order to generate Y .

Remark 1. Note that the resulting cost functions for the CPF and the CFB resemble those of the VAE (Kingma and Welling 2013), the β -VAE (Higgins et al. 2017), the VIB (Alemi et al. 2016), or the nonlinear IB (Kolchinsky, Tracey, and Wolpert 2019). Let us consider the (common) case that the decoder density is estimated with a neural network. If such a network is modified so that it receives as input both the representations and the private or sensitive data instead of only the representations, then the optimization of these algorithms results in private and/or fair representations (see Appendix B for the details).

3 Related Work

3.1 Privacy

If the secret information S is the identity of the samples or their membership to a certain group, the field of *differential privacy* (DP) provides a theoretical framework for defining privacy and several mechanisms able to generate privacy-preserving queries about the data X and explore such data, see, e.g., (Dwork, Roth et al. 2014). If, on the other hand, the secret information is arbitrary, variants of DP such as (Dwork et al. 2006, Bounded DP) and (Kifer and Machanavajjhala 2011, Attribute DP) or the theoretical framework introduced in (du Pin Calmon and Fawaz 2012) are commonly adopted. The privacy funnel (Makhdoumi et al. 2014) is a special case of the latter, when the utility and the privacy are measured with the mutual information.

The original greedy algorithm to compute the PF (Makhdoumi et al. 2014) and other methods that attempt at learning non-parametric encoding densities $p_{Y|X}$ such as (Romanelli, Palamidessi, and Chatzikokolakis 2019) assume the data is discrete or categorical and do not scale. For this reason, approaches that take advantage of the scalability of deep learning emerged. For instance, Edwards and Storkey (2016) and Hamm (2017) learn the representations through adversarial learning but are limited to $S \in \{0, 1\}$ and do not offer an information theoretic interpretation. Similar to us, in the the privacy preserving variational autoencoder (PPVAE) (Nan and Tao 2020) and the unsupervised version of the variational fair autoencoder (VFAE) (Louizos et al. 2016) they learn such representations with variational inference.

At their core, the PPVAE and the unsupervised VFAE end up minimizing the cost functions

$$\begin{aligned} \mathcal{J}_{\text{PPVAE}}(\theta, \phi, \eta) &= \mathbb{E}_{p_{(S, X)}|\theta} [D_{\text{KL}}(p_{Y|(S, X, \theta)} || q_{Y|\theta})] \\ &\quad - \eta^{-1} \mathbb{E}_{p_{(S, X, Y)}|\theta} [\log(q_{X|(S, Y, \phi)})] \end{aligned} \quad (12)$$

and $\mathcal{J}_{\text{VFAE}}(\theta, \phi, \delta) = \mathcal{J}_{\text{PPVAE}}(\theta, \phi, 1) + \delta \mathcal{J}_{\text{MMD}}(\theta, \phi)$, where $\mathcal{J}_{\text{MMD}}(\theta, \phi)$ is a maximum-mean discrepancy term. Even though the resulting function to optimize is similar to ours, it is important to note that the encoding density in these works is $p_{Y|(S, X, \theta)}$, which does not respect the problem’s Markov chain $S \leftrightarrow X \rightarrow Y$. Therefore, the optimization search space includes representations Y that contain information about the private data S that is not even contained in the original data X . Moreover, the private data S is *needed* to generate the representations Y , which is problematic since it might not be available during inference.

3.2 Fairness

The field of algorithmic fairness is mainly dominated by the notions of *individual fairness*, where the sensitive data S is the identity of the data samples, and *group fairness*, where S is a binary variable that represents the membership of the data samples to a certain group. There are several approaches that aim at producing classifiers that ensure either of these notions of fairness; e.g., discrimination-free naive Bayes (Calders, Kamiran, and Pechenizkiy 2009), constrained logistic regression, hinge loss, and support vector machines (Zafar et al. 2017), or regularized logistic regression through the Wasserstein distance (Jiang et al. 2019).

Other lines of work on algorithmic fairness are based on causal inference (Kilbertus et al. 2017; Kusner et al. 2017; Madras et al. 2019) and data massaging (Kamiran and Calders 2010), where the values of the labels of the training data are changed so that the training data is fair.

The notion of fair representations, introduced by Zemel et al. (2013), boosted the advances on algorithmic fairness due to the expressiveness of deep learning. These advances are mainly dominated by adversarial learning (Zemel et al. 2013; Edwards and Storkey 2016; Zhao et al. 2020), even though there are recent variational approaches, too (Louizos et al. 2016; Creager et al. 2019).

The main differences with the variational approach from Creager et al. (2019) are our simple cost function (which

does not require to train an additional adversary discriminator) and that we discard the information that is not necessary to draw inferences about T . They generate two representations, Y_{sens} and $Y_{\text{non-sens}}$, that contain the information about the sensitive data and the original data, respectively, without taking into account the task at hand. At inference time, the sensitive representations Y_{sens} are corrupted with noise or discarded, and thus the non-sensitive representations $Y_{\text{non-sens}}$ from (Creager et al. 2019) serve a similar purpose to the representations Y obtained with our approach. Compared to the *variational fair autoencoder* (Louizos et al. 2016), our encoding density does not require the sensitive information S , which might not be available during inference, thus not breaking the Markov chain $S \leftrightarrow X \rightarrow Y$.

4 Results

In this section, we present experiments on two datasets to showcase the performance of the presented variational approach to the privacy and fairness problems. First, we show the performance in a dataset commonly used for benchmarking both tasks. Second, we show the performance on high-dimensional data on a toy dataset designed for this purpose. The encoder density is modeled with an isotropic Gaussian distribution, i.e., $p_{Y|X,\theta} = \mathcal{N}(Y; \mu_{\text{enc}}(X; \theta), \sigma_{\theta}^2 I_d)$, so that $Y = \mu_{\text{enc}}(X; \theta) + \sigma_{\theta} E$, where $E \sim \mathcal{N}(0, I_d)$, μ_{enc} is a neural network, and d is the dimensionality of the representations. The marginal density of the representations is also modeled as an isotropic Gaussian $q_{Y|\theta} = \mathcal{N}(Y; 0, I_d)$. Finally, the decoder density, $q_{X|(S,Y,\phi)}$ or $q_{T|(S,Y,\phi)}$, is modeled with a product of categorical (for discrete data) and/or isotropic Gaussians (for continuous data), e.g., $q_{X|(S,Y,\phi)} = \text{Cat}(X_1; \rho_{\text{dec}}(Y, S; \phi)) \mathcal{N}(X_2; \mu_{\text{dec}}(S, Y; \phi), \sigma_{\phi}^2)$ if X consists of a discrete variable X_1 and a continuous variable X_2 . The experiments are detailed in Appendix D.

Adult dataset The Adult dataset (available at the UCI machine learning repository (Dua and Graff 2017)) contains 45,222 samples from the 1994 U.S. Census. Each sample comprises 15 features such as, e.g., *gender*, *age*, *income level* (binary variable stating if the income level is higher or lower than \$50,000), or *education level*. For both tasks, we followed the experimental set-up from Zemel et al. (2013), where S is the gender and X is the rest of the features. For the fairness task, we considered T to be the income level.

Toy dataset: Colored MNIST The MNIST dataset (LeCun et al. 1998) is a collection of 70,000 grayscale 28×28 images of hand-written digits from 0 to 9. The Colored MNIST is a modification of the former dataset where each digit is randomly colored in either red, green, or blue. We considered X to be the $3 \times 28 \times 28$ digit images, S to be the color of the digit, and T to be digit’s number.

4.1 Privacy

In the privacy task, the proposed approach is able to control the trade-off between private and informative representations for both the Adult and the Colored MNIST datasets.

We minimized (10) for different values of $\gamma \in [1, 50]$, thus controlling the trade-off between the compression level $I(X; Y)$ and the informativeness of the representations independent of the private data $I(X; Y|S)$, as shown in Figures 3a and 3b. Therefore, as suggested by Proposition 1 and shown in Figures 4a and 4b, it also controls the amount of information the representations keep about the private data, $I(S; Y)$, which was estimated with MINE (Belghazi et al. 2018).

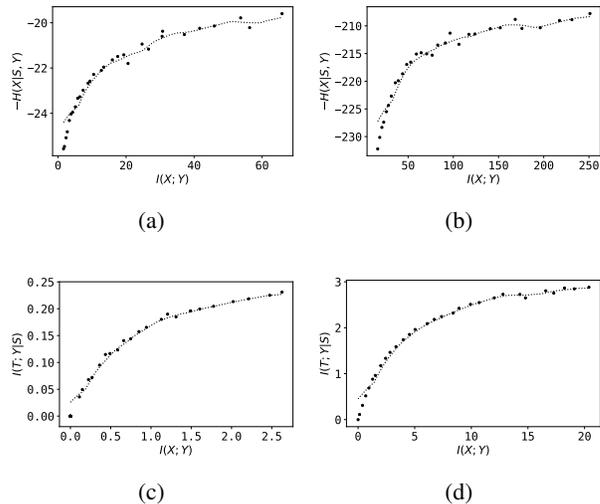


Figure 3: Trade-off between the representations’ compression $I(X; Y)$ and the non-private information retained $I(X; Y|S)$ for the (a) Adult and the (b) colored MNIST datasets with $\gamma \in [1, 50]$. Since $I(X; Y|S) = H(X|S) - H(X|S, Y)$ and $H(X|S)$ does not depend on Y , the reported quantity is $-H(X|S, Y)$. Moreover, trade-off between the compression of the representations $I(X; Y)$ and the non-sensitive information retained about the task $I(T; Y|S)$ for the (c) Adult and the (d) colored MNIST datasets with $\beta \in [1, 50]$. The dots are the computed empirical values and the lines are the moving average of the 1D linear interpolations of such points.

As an illustrative example, we constructed a representation of the same dimensionality, i.e., $3 \times 28 \times 28$, of the hand-written digits by minimizing (10) and setting $\gamma = 1$. This representation is both informative and private, as shown in Figures 5b and 5d. In Figure 5d, the 2-dimensional UMAP (McInnes et al. 2018) vectors of the representations are mingled with respect to their color, as opposed to the UMAP vectors of the original images, where the vectors are clustered by the color of their images (see Figure 5c).

Compared to the variational approaches to the PF (Nan and Tao 2020, PPVAE) and (Louizos et al. 2016, VFAE), the proposed approach performed better in terms of information leakage $I(S; Y)$ and accuracy of non-linear attackers (see Table 1). More specifically, the leaked mutual information is about an order of magnitude lower than the obtained in the other methods and the accuracy of a random forest attacker

is below the prior probability (0.67), while the other methods allow successful attacks of 0.8 – 0.9 accuracy. A possible explanation for this phenomenon is that some information about S is leaked to Y via the encoding density $p_{Y|(S,X,\theta)}$, which does not respect the Markov chain $S \leftrightarrow X \rightarrow Y$.

Table 1: Random forest attacker’s accuracy and mutual information between the sensitive S and representation Y variables on the Adult dataset. The PPVAE and VFAE parameter ranges are $\eta^{-1} \in [1, 50]$ and $\delta \in [N_{\text{batch}}, 1000N_{\text{batch}}]$.

Methods	Attacker’s accuracy (S)	$I(S; Y)$
Ours	0.60 – 0.64	0.01 – 0.08
PPVAE	0.79 – 0.93	0.29 – 0.63
VFAE	0.81 – 0.95	0.28 – 0.44

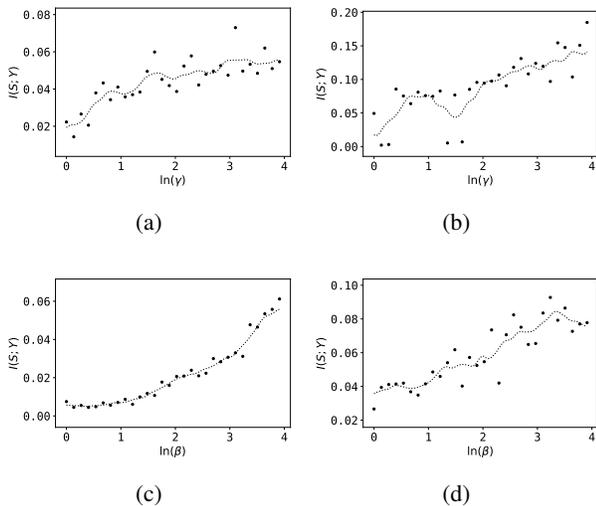


Figure 4: Behavior of the private information $I(S; Y)$ kept by the private representations in the (a) Adult and (b) the Colored MNIST datasets with $\gamma \in [1, 50]$; and by the fair representations in the (c) Adult and (d) the Colored MNIST datasets with $\beta \in [1, 50]$. The dots are the computed empirical values and the lines are the moving average of the 1D linear interpolations of such points.

4.2 Fairness

In the fairness task, our proposed variational approach is also able to control the trade-off between fair and accurate representations. We minimized (11) for different values of $\beta \in [1, 50]$, thus controlling the trade-off between the compression level $I(X; Y)$ and the predictability without the sensitive variable $I(T; Y|S)$, as shown in Figures 3c and 3d. Moreover, as suggested by Proposition 2 and shown in Figures 4c and 4d, we also control amount of information that the representations retain about the sensitive data $I(S; Y)$, which was estimated with MINE (Belghazi et al. 2018).

Furthermore, in the Adult dataset, the Lagrange multiplier β allows us to control the behavior of different utility and

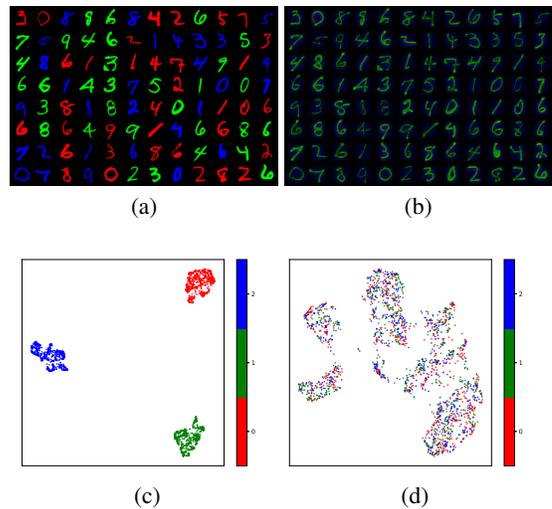


Figure 5: Random samples of Colored MNIST (a) original data and (b) private representations and their UMAP dimensionality reduction (c and d, respectively). In the UMAP dimensionality reduction, each vector point is colored with the same color the digit was. Results obtained for $\gamma = 1$.

group fairness indicators (defined in Appendix E), namely the accuracy, the error gap, and the discrimination (or demographic parity gap). That is, the higher the value of β , the higher the accuracy and the discrimination, and the lower the error gap (Figures 6a, 6b, and 6d). The behavior of the discrimination is enforced by the minimization of $I(S; Y)$, as discussed in Remark 4 from Appendix E. However, there is no clear indication of the effect of β on the accuracy of adversarial predictors on the sensitive data (which is still below the prior probability of the biased training dataset) and on the equalized odds (Figures 6e and 6c). The equalized odds are not optimized in this scenario since the resulting representations Y are such that $I(S; Y; T) < 0$ as discussed in Remark 5 from Appendix E. An example when the equalized odds gap is minimized is presented in Appendix D.

The representations generated from the proposed method are more robust to non-linear adversaries (as shown in Table 2 by the smaller accuracy on S and smaller discrimination when the adversary employs a random forest) than the standard baseline from Zemel et al. (2013, LFR). Compared with other state-of-the-art methods, either those which employ variational inference (Creager et al. 2019, FFVAE) or adversarial training (Zhao et al. 2020, CFAIR), the proposed method for generating fair representations achieves similar results (as shown in Table 2), albeit having an easier cost function and requiring to train less networks, respectively.

5 Discussion

In this article, we studied the problem of mitigating the leakage of private or sensitive information S into data-driven systems through the training data X . We formalized the trade-off between the relevant information for the system that is not shared by the private or sensitive data S and the

Table 2: Fairness metrics with different methods on Adult dataset. Displayed as: Logistic regression / Random forest. The best hyperparameters for the other methods have been selected (see Appendix D). These models and compared to our model with the hyperparameters that reaches the most similar performance.

Methods	Accuracy (T)	Accuracy (S)	Discrimination	Error gap	EO gap
LFR (Zemel et al. 2013)	0.84 / 0.84	0.66 / 0.98	0.07 / 0.16	0.10 / 0.12	0.18 / 0.07
Ours ($\beta = 17.0$)	0.82 / 0.80	0.66 / 0.62	0.08 / 0.08	0.12 / 0.13	0.09 / 0.09
FFVAE (Creager et al. 2019, $\alpha = 200$)	0.77 / 0.75	0.67 / 0.61	0.00 / 0.01	0.17 / 0.12	0.04 / 0.04
CFAIR (Zhao et al. 2020, $\lambda = 1000$)	0.77 / 0.71	0.69 / 0.65	0.02 / 0.01	0.17 / 0.12	0.02 / 0.04
Ours ($\beta = 1.96$)	0.76 / 0.72	0.67 / 0.61	0.00 / 0.00	0.19 / 0.15	0.00 / 0.00

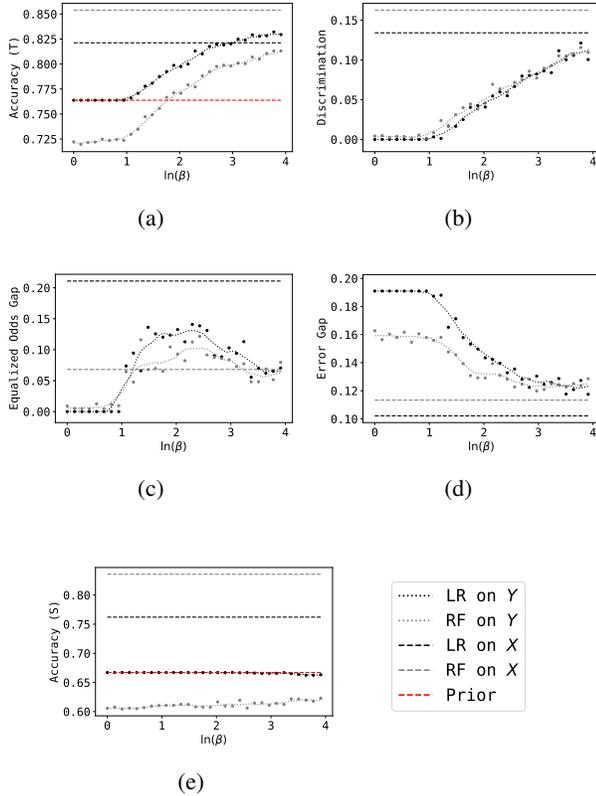


Figure 6: Behavior of (a) the accuracy on T , (b) the discrimination, (c) the equalized odds gap, (d) the error gap, and (e) the accuracy on S of a logistic regression (LR, in black) and a random forest (RF, in gray) of the fair representations (dots and dotted line) and the original data (dashed line) learned with $\beta \in [1, 50]$ on the Adult dataset. The dashed line in red is the accuracy of a prior-based classifier.

remaining information as a constrained optimization problem. When the task of the system is known, the problem is referred to as learning fair representations and the formalization is the conditional fairness bottleneck (CFB); and when the task is unknown, the problem is referred to as learning private representations and the formalization is the conditional privacy funnel (CPF).

We proposed a variational approach, based on the Lagrangians of the CPF and the CFB, to solve the problem. This approach leads to a simple structure where the tasks of learning private and/or fair representations can be easily identified. Moreover, in practice, private and fair representations can be learned with little modification to the implementation of common algorithms such as the VAE (Kingma and Welling 2013), the β -VAE (Higgins et al. 2017), the VIB (Alemi et al. 2016), or the nonlinear IB (Kolchinsky, Tracey, and Wolpert 2019). Namely, modifying the decoder neural network so it receives both the representation Y and the private or sensitive data S as an input. Then, the learned representations can be fed to any algorithm of choice. For this reason, the efforts for reducing unfair decisions and privacy breaches will be small for many practitioners.

5.1 Limitations and future directions

Problem formulation The CPF and the CFB as defined in (1) and (2) are non-convex optimization problems with respect to $P_{Y|X}$. More specifically, they are a minimization of a convex function with non-convex constraints (see Appendix C). Therefore, (i) the optimal conditional distribution $P_{Y|X}^*$ that minimizes the Lagrangian might not be achieved through gradient descent, and (ii) even if $P_{Y|X}^*$ is achieved, it could be a sub-optimal value for (1) or (2), since the problems are not *strongly dual* (Boyd, Boyd, and Vandenberghe 2004, Section 5.2.3). A possible solution could be the application of a monotonically increasing concave function u to $I(X; Y|S)$ or $I(T; Y|S)$ in the CPF or CFB Lagrangians, respectively, so that $u(I(X; Y|S))$ or $u(I(T; Y|S))$ is concave (and hence the Lagrangian is convex) in the domain of interest. For some u , this approach might allow to attain the desired r in (1) or (2) with a specific value of the Lagrange multiplier; see (Rodríguez Gálvez, Thobaben, and Skoglund 2020) for an example of this approach for the IB.

Proposed approach The proposed approach entails two limitations that are common in variational attempts at solving an optimization problem. Namely: (i) it approximates the decoding and the marginal distributions and (ii) it considers parametrized densities. The first issue restricts the search space of the possible encoding distributions $P_{Y|X}$ to those distributions with a decoding and marginal distributions that follow the restrictions of the variational approximation. The second issue further limits the search space to the obtain-

able encoding distributions with densities $p_{Y|(X,\theta)}$ with a parametrization θ . For this reason, richer encoding distributions and marginals, e.g., by means of normalizing flows (Rezende and Mohamed 2015; Kingma et al. 2016), are a possible direction to mitigate these issues.

Potential Ethical Impact

Privacy breaches and unfairness are concerning problems that often arise in (learning) algorithms. Moreover, aside from the realm of algorithms, these are problems that humans, as a society, aim to mitigate in our objective to reach sustainability (United Nations 2016, Goal 10). With the present paper, we contribute towards the development of privacy-preserving and fair systems, thus contributing to a sustainable development. For example, privacy-preserving and fair decision-making algorithms could directly contribute to the UN’s targets 10.2 and 10.3 (United Nations 2016, Targets 10.2 and 10.3), namely, “empower and promote the social, economic, and political inclusion of all, irrespective of age, sex, disability, race, ethnicity, origin, religion, or economic or other status” and “ensure equal opportunity and reduce inequalities of outcome, including by eliminating discriminatory laws, policies, and practices and promoting appropriate legislation, policies, and action in this regard”, respectively.

Even though our contribution will not help to directly level out social, political, and economic inequalities, the results and algorithms provided in this paper will help to avoid that inequalities will be amplified and prolonged through data-driven services and decision mechanisms (e.g., for insurances, administration, banking, or loans). By treating the data entered into such services and systems fairly and confidentially, as enforced by the proposed approach of this paper, our contribution has the potential to empower and promote social and economical inclusion (United Nations 2016, Target 10.2) and ensure equal opportunity (United Nations 2016, Target 10.3) in this specific domain of people’s everyday life. Furthermore, we believe that our results are likely to be adopted by algorithm designers and practitioners, as our solutions can easily be integrated into existing standard representation learning algorithms as noted in Remark 1 and detailed in Appendix B.

References

- Achille, A.; and Soatto, S. 2018. Emergence of invariance and disentanglement in deep representations. *The Journal of Machine Learning Research* 19(1): 1947–1980.
- Alemi, A. A.; Fischer, I.; Dillon, J. V.; and Murphy, K. 2016. Deep variational information bottleneck. *International Conference on Learning Representations (ICLR)*.
- Belghazi, M. I.; Baratin, A.; Rajeshwar, S.; Ozair, S.; Bengio, Y.; Courville, A.; and Hjelm, D. 2018. Mutual information neural estimation. In *International Conference on Machine Learning (ICML)*, 531–540.
- Boyd, S.; Boyd, S. P.; and Vandenberghe, L. 2004. *Convex optimization*. Cambridge university press.
- Calders, T.; Kamiran, F.; and Pechenizkiy, M. 2009. Building classifiers with independency constraints. In *2009 IEEE International Conference on Data Mining Workshops*, 13–18. IEEE.
- Chatzikokolakis, K.; Chothia, T.; and Guha, A. 2010. Statistical measurement of information leakage. In *International Conference on Tools and Algorithms for the Construction and Analysis of Systems*, 390–404. Springer.
- Chen, T. Q.; Li, X.; Grosse, R. B.; and Duvenaud, D. K. 2018. Isolating sources of disentanglement in variational autoencoders. In *Advances in Neural Information Processing Systems (NeurIPS)*, 2610–2620.
- Chouldechova, A.; and Roth, A. 2018. The frontiers of fairness in machine learning. *arXiv preprint arXiv:1810.08810*.
- Corbett-Davies, S.; and Goel, S. 2018. The measure and mismeasure of fairness: A critical review of fair machine learning. *arXiv preprint arXiv:1808.00023*.
- Cover, T. M.; and Thomas, J. A. 2006. *Elements of information theory*. John Wiley & Sons, second edition edition.
- Creager, E.; Madras, D.; Jacobsen, J.-H.; Weis, M.; Swersky, K.; Pitassi, T.; and Zemel, R. 2019. Flexibly Fair Representation Learning by Disentanglement. In *International Conference on Machine Learning (ICML)*, 1436–1445.
- Dieterich, W.; Mendoza, C.; and Brennan, T. 2016. COMPAS risk scales: Demonstrating accuracy equity and predictive parity. *Northpointe Inc*.
- du Pin Calmon, F.; and Fawaz, N. 2012. Privacy against statistical inference. In *Allerton Conference on Communication, Control, and Computing (Allerton)*, 1401–1408. IEEE.
- Dua, D.; and Graff, C. 2017. UCI Machine Learning Repository. URL <http://archive.ics.uci.edu/ml>.
- Dwork, C.; Hardt, M.; Pitassi, T.; Reingold, O.; and Zemel, R. 2012. Fairness through awareness. In *Proceedings of the 3rd Innovations in Theoretical Computer Science conference*, 214–226.
- Dwork, C.; McSherry, F.; Nissim, K.; and Smith, A. 2006. Calibrating noise to sensitivity in private data analysis. In *Theory of cryptography conference*, 265–284. Springer.
- Dwork, C.; Roth, A.; et al. 2014. The algorithmic foundations of differential privacy. *Foundations and Trends® in Theoretical Computer Science* 9(3–4): 211–407.
- Edwards, H.; and Storkey, A. 2016. Censoring representations with an adversary. *International Conference on Learning Representations (ICLR)*.
- Fischer, I. 2020. The Conditional Entropy Bottleneck. *arXiv preprint arXiv:2002.05379*.
- Ganin, Y.; Ustinova, E.; Ajakan, H.; Germain, P.; Larochelle, H.; Laviolette, F.; Marchand, M.; and Lempitsky, V. 2016. Domain-adversarial training of neural networks. *The Journal of Machine Learning Research* 17(1): 2096–2030.
- Hamm, J. 2017. Minimax filter: learning to preserve privacy from inference attacks. *The Journal of Machine Learning Research* 18(1): 4704–4734.

- Hardt, M.; Price, E.; and Srebro, N. 2016. Equality of opportunity in supervised learning. In *Advances in Neural Information Processing Systems (NeurIPS)*, 3315–3323.
- Harris, C. R.; Millman, K. J.; van der Walt, S. J.; Gommers, R.; Virtanen, P.; Cournapeau, D.; Wieser, E.; Taylor, J.; Berg, S.; Smith, N. J.; et al. 2020. Array programming with NumPy. *Nature* 585(7825): 357–362.
- Higgins, I.; Matthey, L.; Pal, A.; Burgess, C.; Glorot, X.; Botvinick, M.; Mohamed, S.; and Lerchner, A. 2017. Beta-VAE: Learning Basic Visual Concepts with a Constrained Variational Framework. *International Conference on Learning Representations (ICLR)*.
- Hjelm, R. D.; Fedorov, A.; Lavoie-Marchildon, S.; Grewal, K.; Bachman, P.; Trischler, A.; and Bengio, Y. 2018. Learning deep representations by mutual information estimation and maximization. In *International Conference on Learning Representations (ICLR)*.
- Issa, I.; Wagner, A. B.; and Kamath, S. 2019. An operational approach to information leakage. *IEEE Transactions on Information Theory* 66(3): 1625–1657.
- Jiang, R.; Pacchiano, A.; Stepleton, T.; Jiang, H.; and Chippa, S. 2019. Wasserstein fair classification. *Conference on Uncertainty in Artificial Intelligence (UAI)*.
- Kamiran, F.; and Calders, T. 2010. Classification with no discrimination by preferential sampling. In *Proceedings of the 19th Machine Learning Conference of Belgium and The Netherlands*, 1–6. Citeseer.
- Kifer, D.; and Machanavajjhala, A. 2011. No free lunch in data privacy. In *Proceedings of the 2011 ACM SIGMOD International Conference on Management of data*, 193–204.
- Kilbertus, N.; Carulla, M. R.; Parascandolo, G.; Hardt, M.; Janzing, D.; and Schölkopf, B. 2017. Avoiding discrimination through causal reasoning. In *Advances in Neural Information Processing Systems (NeurIPS)*, 656–666.
- Kim, H.; and Mnih, A. 2018. Disentangling by Factorising. In *International Conference on Machine Learning (ICML)*, 2649–2658.
- Kingma, D. P.; and Ba, J. 2014. Adam: A method for stochastic optimization. *arXiv preprint arXiv:1412.6980*.
- Kingma, D. P.; Salimans, T.; Jozefowicz, R.; Chen, X.; Sutskever, I.; and Welling, M. 2016. Improved variational inference with inverse autoregressive flow. In *Advances in Neural Information Processing Systems (NeurIPS)*, 4743–4751.
- Kingma, D. P.; and Welling, M. 2013. Auto-encoding variational Bayes. *arXiv preprint arXiv:1312.6114*.
- Kolchinsky, A.; Tracey, B. D.; and Wolpert, D. H. 2019. Nonlinear information bottleneck. *Entropy* 21(12): 1181.
- Kusner, M. J.; Loftus, J.; Russell, C.; and Silva, R. 2017. Counterfactual fairness. In *Advances in Neural Information Processing Systems (NeurIPS)*, 4066–4076.
- LeCun, Y.; Bottou, L.; Bengio, Y.; and Haffner, P. 1998. Gradient-based learning applied to document recognition. *Proceedings of the IEEE* 86(11): 2278–2324.
- Louizos, C.; Swersky, K.; Li, Y.; Welling, M.; and Zemel, R. 2016. The variational fair autoencoder. *International Conference on Learning Representations (ICLR)*.
- Madras, D.; Creager, E.; Pitassi, T.; and Zemel, R. 2019. Fairness through causal awareness: Learning causal latent-variable models for biased data. In *Proceedings of the Conference on Fairness, Accountability, and Transparency*, 349–358.
- Makhdoumi, A.; Salamatian, S.; Fawaz, N.; and Médard, M. 2014. From the information bottleneck to the privacy funnel. In *IEEE Information Theory Workshop (ITW)*, 501–505. IEEE.
- McInnes, L.; Healy, J.; Saul, N.; and Großberger, L. 2018. UMAP: Uniform Manifold Approximation and Projection. *Journal of Open Source Software* 3(29).
- Nan, L.; and Tao, D. 2020. Variational approach for privacy funnel optimization on continuous data. *Journal of Parallel and Distributed Computing* 137: 17–25.
- Paszke, A.; Gross, S.; Massa, F.; Lerer, A.; Bradbury, J.; Chanan, G.; Killeen, T.; Lin, Z.; Gimelshein, N.; Antiga, L.; et al. 2019. Pytorch: An imperative style, high-performance deep learning library. In *Advances in neural information processing systems*, 8026–8037.
- Pedregosa, F.; Varoquaux, G.; Gramfort, A.; Michel, V.; Thirion, B.; Grisel, O.; Blondel, M.; Prettenhofer, P.; Weiss, R.; Dubourg, V.; Vanderplas, J.; Passos, A.; Cournapeau, D.; Brucher, M.; Perrot, M.; and Duchesnay, E. 2011. Scikit-learn: Machine Learning in Python. *Journal of Machine Learning Research* 12: 2825–2830.
- Rahimi, A.; and Recht, B. 2009. Weighted sums of random kitchen sinks: Replacing minimization with randomization in learning. In *Advances in neural information processing systems (NeurIPS)*, 1313–1320.
- Rezende, D. J.; and Mohamed, S. 2015. Variational inference with normalizing flows. *arXiv preprint arXiv:1505.05770*.
- Rodríguez Gálvez, B.; Thobaben, R.; and Skoglund, M. 2020. The Convex Information Bottleneck Lagrangian. *Entropy* 22(1): 98.
- Romanelli, M.; Palamidessi, C.; and Chatzikokolakis, K. 2019. Generating optimal privacy-protection mechanisms via machine learning. *arXiv preprint arXiv:1904.01059*.
- Tishby, N.; Pereira, F. C.; and Bialek, W. 2000. The information bottleneck method. *arXiv preprint physics/0004057*.
- United Nations. 2016. Transforming our world: The 2030 agenda for sustainable development.
- Wainwright, M. 2019. *High-Dimensional Statistics*. Cambridge University Press.
- Yeung, R. W. 1991. A new outlook on Shannon’s information measures. *IEEE Transactions on Information Theory* 37(3): 466–474.
- Zafar, M. B.; Valera, I.; Rodriguez Gomez, M.; and Gummadi, K. P. 2017. Fairness constraints: Mechanisms for fair

classification. *International Conference on Artificial Intelligence and Statistics (AISTATS)* .

Zemel, R.; Wu, Y.; Swersky, K.; Pitassi, T.; and Dwork, C. 2013. Learning fair representations. In *International Conference on Machine Learning (ICML)*, 325–333.

Zhao, H.; Coston, A.; Adel, T.; and Gordon, G. J. 2020. Conditional learning of fair representations. *International Conference on Learning Representations (ICLR)* .

Zhao, H.; and Gordon, G. 2019. Inherent tradeoffs in learning fair representations. In *Advances in Neural Information Processing Systems (NeurIPS)*, 15649–15659.

Zhao, S.; Song, J.; and Ermon, S. 2019. Infovae: Balancing learning and inference in variational autoencoders. In *Proceedings of the Thirty-Third AAAI Conference on Artificial Intelligence*, volume 33, 5885–5892.

Zhu, Y.; and Bettati, R. 2005. Anonymity vs. information leakage in anonymity systems. In *25th IEEE International Conference on Distributed Computing Systems (ICDCS'05)*, 514–524. IEEE.

Technical Appendix

A Equivalences of the Lagrangians

In this section of the appendix, we show how minimizing the Lagrangians of the CPF and the CFB problems is equivalent to minimizing other Lagrangians. First, in A.1 we show it is equivalent to minimizing the Lagrangians that are used in the variational approach we propose in this paper. Then, in A.2 we show that minimizing the Lagrangian of the CPF is equivalent to minimizing the Lagrangian of the PF, meaning that the conditional probability distributions $P_{Y|X}$ obtained using the Lagrangian of the CPF could have been obtained through the Lagrangian of the PF, too.

A.1 Equivalence of the Lagrangians used for the minimization

Proposition 1. *Minimizing $\mathcal{L}_{\text{CPF}}(P_{Y|X}, \lambda)$ is equivalent to minimizing $\mathcal{J}_{\text{CPF}}(P_{Y|X}, \gamma)$, where $\gamma = \lambda + 1$ and*

$$\mathcal{J}_{\text{CPF}}(P_{Y|X}, \gamma) = I(X; Y) - \gamma I(X; Y|S). \quad (5)$$

Proof. If we manipulate the expression of the CPF Lagrangian we can see how minimizing $\mathcal{L}_{\text{CPF}}(P_{Y|X}, \lambda)$ is equivalent to minimizing $\mathcal{J}_{\text{CPF}}(P_{Y|X}, \gamma)$, where $\gamma = \lambda + 1$. More specifically,

$$\begin{aligned} & \arg \inf_{P_{Y|X} \in \mathcal{P}} \{ \mathcal{L}_{\text{CPF}}(P_{Y|X}, \lambda) \} \\ &= \arg \inf_{P_{Y|X} \in \mathcal{P}} \{ I(S; Y) - \lambda I(X; Y|S) \} \end{aligned} \quad (13)$$

$$= \arg \inf_{P_{Y|X} \in \mathcal{P}} \{ I(X; Y) - I(X; Y|S) - \lambda I(X; Y|S) \} \quad (14)$$

$$= \arg \inf_{P_{Y|X} \in \mathcal{P}} \{ I(X; Y) - (\lambda + 1) I(X; Y|S) \} \quad (15)$$

$$= \arg \inf_{P_{Y|X} \in \mathcal{P}} \{ \mathcal{J}_{\text{CPF}}(P_{Y|X}, \lambda + 1) \}, \quad (16)$$

where \mathcal{P} is the set of probability distributions over \mathcal{Y} such that if $P_{Y|X=x} \in \mathcal{P}$ for all $x \in \mathcal{X}$, then the Markov chain $S \leftrightarrow X \rightarrow Y$ holds. \square

Proposition 2. *Minimizing $\mathcal{L}_{\text{CFB}}(P_{Y|X}, \lambda)$ is equivalent to minimizing $\mathcal{J}_{\text{CFB}}(P_{Y|X}, \beta)$, where $\beta = \lambda + 1$ and*

$$\mathcal{J}_{\text{CFB}}(P_{Y|X}, \beta) = I(X; Y) - \beta I(T; Y|S). \quad (6)$$

Proof. If we manipulate the expression of the CFB Lagrangian we can see how minimizing $\mathcal{L}_{\text{CFB}}(P_{Y|X}, \lambda)$ is equivalent to minimizing $\mathcal{J}_{\text{CFB}}(P_{Y|X}, \beta)$, where $\beta = \lambda + 1$.

More specifically,

$$\begin{aligned} & \arg \inf_{P_{Y|X} \in \mathcal{P}} \{ \mathcal{L}_{\text{CFB}}(P_{Y|X}, \lambda) \} \\ &= \arg \inf_{P_{Y|X} \in \mathcal{P}} \{ I(S; Y) + I(X; Y|S, T) - \lambda I(T; Y|S) \} \end{aligned} \quad (17)$$

$$= \arg \inf_{P_{Y|X} \in \mathcal{P}} \{ I(X; Y) - I(T; Y|S) - \lambda I(T; Y|S) \} \quad (18)$$

$$= \arg \inf_{P_{Y|X} \in \mathcal{P}} \{ I(X; Y) - (\lambda + 1) I(T; Y|S) \} \quad (19)$$

$$= \arg \inf_{P_{Y|X} \in \mathcal{P}} \{ \mathcal{J}_{\text{CFB}}(P_{Y|X}, \lambda + 1) \}, \quad (20)$$

where \mathcal{P} is the set of probability distributions over \mathcal{Y} such that if $P_{Y|X=x} \in \mathcal{P}$ for all $x \in \mathcal{X}$, then the Markov chains $S \leftrightarrow X \rightarrow Y$ and $T \leftrightarrow X \rightarrow Y$ hold. \square

A.2 Equivalence of the Lagrangians of the privacy funnel and the CPF

The privacy funnel is defined in a similar way to the CPF. It is an optimization problem that tries to design an encoding probability distribution $P_{Y|X}$ such that the representation Y keeps a certain level r' of information about the data of interest X , while minimizing the information it keeps about the private data S (Makhdoumi et al. 2014). That is,

$$\arg \inf_{P_{Y|X}} \{ I(S; Y) \} \text{ s.t. } I(X; Y) \geq r'. \quad (21)$$

Therefore, the Lagrangian of the privacy funnel problem is

$$\mathcal{L}_{\text{PF}}(P_{Y|X}, \alpha) = I(S; Y) - \alpha I(X; Y), \quad (22)$$

where $\alpha \in [0, 1]$ is the Lagrange multiplier of $\mathcal{L}_{\text{PF}}(P_{Y|X}, \alpha)$.¹ This multiplier controls the trade-off between the information the representations keep about the private and the original data.

Proposition 3. *Minimizing $\mathcal{L}_{\text{CPF}}(P_{Y|X}, \lambda)$ is equivalent to minimizing $\mathcal{L}_{\text{PF}}(P_{Y|X}, \alpha)$, where $\alpha = \lambda / (\lambda + 1)$.*

Proof. If we manipulate the expression of the CPF Lagrangian we can see how the minimizing $\mathcal{L}_{\text{CPF}}(P_{Y|X}, \lambda)$ is equivalent to minimizing $\mathcal{L}_{\text{PF}}(P_{Y|X}, \alpha)$, where $\alpha = \lambda / (\lambda + 1)$. More specifically,

¹If $\alpha = 1$, then $\mathcal{L}_{\text{PF}}(P_{Y|X}, 1) = -I(X; Y|S)$, for which optimal values of the encoding distribution $P_{Y|X}$ can filter private information arbitrarily. If $\alpha > 1$ this problem is even more pronounced. For $\alpha \leq 0$ trivial encoding distributions like a degenerate distribution $P_{Y|X}$ with density $p_{Y|X} = \delta(Y)$ are minimizers of the Lagrangian.

$$\begin{aligned} & \arg \inf_{P_{Y|X} \in \mathcal{P}} \{ \mathcal{L}_{\text{CPF}}(P_{Y|X}, \lambda) \} \\ &= \arg \inf_{P_{Y|X} \in \mathcal{P}} \{ I(S; Y) - \lambda I(X; Y|S) \} \end{aligned} \quad (23)$$

$$= \arg \inf_{P_{Y|X} \in \mathcal{P}} \{ I(S; Y) - \lambda (I(X; Y) - I(S; Y)) \} \quad (24)$$

$$= \arg \inf_{P_{Y|X} \in \mathcal{P}} \{ (\lambda + 1)I(S; Y) - \lambda I(X; Y) \} \quad (25)$$

$$= \arg \inf_{P_{Y|X} \in \mathcal{P}} \left\{ (\lambda + 1) \left(I(S; Y) - \frac{\lambda}{\lambda + 1} I(X; Y) \right) \right\} \quad (26)$$

$$= \arg \inf_{P_{Y|X} \in \mathcal{P}} \left\{ \mathcal{L}_{\text{PF}} \left(P_{Y|X}, \frac{\lambda}{\lambda + 1} \right) \right\}, \quad (27)$$

where \mathcal{P} is the set of probability distributions over \mathcal{Y} such that if $P_{Y|X=x} \in \mathcal{P}$ for all $x \in \mathcal{X}$, then the Markov chain $S \leftrightarrow X \rightarrow Y$ holds. \square

We note how the relationship $\alpha = \lambda/(\lambda + 1)$ maintains $\alpha \in [0, 1)$ for $\lambda \geq 0$. This showcases how the CPF poses a more restrictive problem, in the sense that as long as $\lambda < \infty$ there are no solutions of the problem that filter private information arbitrarily.

B Modification of common algorithms to obtain private and/or fair representations

In this section of the appendix, we discuss the simple changes needed to common representation learning algorithms to implement our proposed variational approach. First, we show how common unsupervised learning algorithms can be modified to the variational approach to the CPF, thus generating private representations. Then, we show how common supervised learning algorithms can be modified to the variational approach to the CFB, thus generating fair representations.

Common unsupervised learning algorithms. The cost function of the β -VAE (Higgins et al. 2017) and the VIB (Alemi et al. 2016) (when the target variable is the identity of the samples) is

$$\begin{aligned} \mathcal{F}_{\text{uns}}(\theta, \phi, \eta) &= \frac{1}{N} \sum_{i=1}^N D_{\text{KL}}(p_{Y|(X=x^{(i)}, \theta)} || q_{Y|\theta}) \\ &\quad - \eta^{-1} \mathbb{E}_{p_E} \left[\log \left(q_{X|(Y=f(x^{(i)}, E), \phi)}(x^{(i)}) \right) \right], \end{aligned} \quad (28)$$

where η is a parameter that controls the trade-off between the compression of the representations Y and their ability to reconstruct the original data X . Similarly, the VAE (Kingma and Welling 2013) cost function is $\mathcal{F}_{\text{uns}}(\theta, \phi, 1)$.

Comparison with the CPF. If we compare (28) with the cost function of the CPF $\tilde{\mathcal{J}}_{\text{CPF}}(\theta, \phi, \gamma)$, we observe that the only difference (provided that $\eta^{-1} = \gamma$) is the decoding density. In the CPF the decoding density of the original data

X depends both on the representations Y and on the private data S , while in (28) it only depends on the representations Y . Therefore, the cost function $\mathcal{F}_{\text{uns}}(\theta, \phi, \eta)$ is recovered from the cost function of the CPF in the case that $q_{X|(S, Y, \phi)} = q_{X|(Y, \phi)}$. However, this is not desirable, since it means that the representations Y contain all the information from the private data S necessary to reconstruct X .

Modifications to obtain private representations. In these unsupervised learning algorithms (Kingma and Welling 2013; Higgins et al. 2017; Alemi et al. 2016) the decoding (or generative) density is parametrized with neural networks, e.g., $q_{X|(Y, \phi)} = \text{Cat}(X; \rho_{\text{dec}}(Y; \phi))$ if X is discrete and $q_{X|(Y, \phi)} = \mathcal{N}(X; \mu_{\text{dec}}(Y; \phi), \sigma_{\text{dec}}(Y; \phi)^2 I_{d_{\text{dec}}})$ if X is continuous, where $\rho_{\text{dec}}, \mu_{\text{dec}}$, and σ_{dec} are neural networks and d_{dec} is the dimensionality of X . In this work, the decoding density can also be parametrized with neural networks, e.g., $\text{Cat}(X; \rho'_{\text{dec}}(S, Y; \phi))$ if X is discrete and $q_{X|(Y, \phi)} = \mathcal{N}(X; \mu'_{\text{dec}}(S, Y; \phi), \sigma'_{\text{dec}}(S, Y; \phi)^2 I_{d_{\text{dec}}})$ if X is continuous, where $\rho'_{\text{dec}}, \mu'_{\text{dec}}$, and σ'_{dec} are neural networks. Therefore, if the decoding density neural networks from (Kingma and Welling 2013; Higgins et al. 2017; Alemi et al. 2016) are modified so that they take the private data S as an input, then the resulting algorithm is the one proposed in this paper.

Common supervised learning algorithms. The cost function of the VIB (Alemi et al. 2016) and the nonlinear IB (Kolchinsky, Tracey, and Wolpert 2019) is

$$\begin{aligned} \mathcal{F}_{\text{sup}}(\theta, \phi, \eta) &= \frac{1}{N} \sum_{i=1}^N D_{\text{KL}}(p_{Y|(X=x^{(i)}, \theta)} || q_{Y|\theta}) \\ &\quad - \eta^{-1} \mathbb{E}_{p_E} \left[\log \left(q_{T|(Y=f(x^{(i)}, E), \phi)}(t^{(i)}) \right) \right], \end{aligned} \quad (29)$$

where η is a parameter that controls the trade-off between the compression of the representations Y and their ability to draw inferences about the task T .

Comparison with the CFB. Similarly to the comparison of the unsupervised learning algorithms and the CPF, we observe that (29) only differs with the cost function $\tilde{\mathcal{J}}_{\text{CFB}}(\theta, \phi, \beta)$ in the decoding density, i.e., the cost function $\mathcal{F}_{\text{sup}}(\theta, \phi, \eta)$ can be recovered from $\tilde{\mathcal{J}}_{\text{CFB}}(\theta, \phi, \beta)$ by setting $q_{T|(S, Y, \phi)} = q_{T|(Y, \phi)}$. The inference density of the task T only depends on the representations Y in (Alemi et al. 2016; Kolchinsky, Tracey, and Wolpert 2019), while in our work it depends both on the representations Y and the sensitive data S . Hence, in these works the representations contain all the information from the sensitive data S necessary to draw inferences about the task T .

Modifications to obtain fair representations. The argument is analogous to the one for the modifications of unsupervised learning algorithms to obtain private representations. The only modification required in these supervised learning algorithms (Alemi et al. 2016; Kolchinsky, Tracey,

and Wolpert 2019) is to modify the decoding density neural networks to receive the sensitive data S as an input as well as the representations Y .

Invariants of the algorithms. In all these works (Kingma and Welling 2013; Higgins et al. 2017; Alemi et al. 2016; Kolchinsky, Tracey, and Wolpert 2019) and ours, the first (or the compression) term is usually calculated assuming that the encoder density is parametrized with neural networks, e.g., $p_{Y|(X,\theta)} = \mathcal{N}(Y; \mu_{\text{enc}}(X; \theta), \sigma_{\text{enc}}(X; \theta)^2 I_d)$, which allows the representations to be constructed using the reparametrization trick, e.g., $Y = \mu_{\text{enc}}(X; \theta) + \sigma_{\text{enc}}(X; \theta)E$, where $E \sim \mathcal{N}(0, I_d)$, d is the dimensionality of the representations, and I_d is the d -dimensional identity matrix. Then, the marginal density of the representations is set so that the Kullback-Leibler divergence has either a closed expression, a simple way to estimate it, or a simple upper bound, e.g., $q_{Y|\theta} = \mathcal{N}(Y; 0, I_d)$ or $q_{Y|\theta} = \frac{1}{N} \sum_{i=1}^N p_{Y|(X=x^{(i)}, \theta)}$, where $x^{(i)}$ are the input data samples. Moreover, the loss function applied to the output of the decoding density and the optimization algorithm, e.g., stochastic gradient descent or Adam (Kingma and Ba 2014), can remain the same in these works and ours, too.

Remark 2. *The aforementioned modifications can also be introduced in other algorithms with cost functions with additional terms to \mathcal{F}_{uns} and \mathcal{F}_{sup} . For example, adding a maximum-mean discrepancy (MMD) term on the representation priors to avoid the information preference problem like in the InfoVAE (Zhao, Song, and Ermon 2019); adding an MMD term on the encoder densities to enforce privacy or fairness like in the VFAE (Louizos et al. 2016); or adding a total correlation penalty to the representation’s marginal to enforce disentangled representations like in the Factor-VAE, the β -TCVAE, or the FFVAE (Kim and Mnih 2018; Chen et al. 2018; Creager et al. 2019).*

C Non-convexity of the CPF and the CFB

In this section of the appendix, we show how both the CPF and the CFB as defined in (1) and (2) are non-convex optimization problems.

Lemma 1. *Let $X \in \mathcal{X}$, $S \in \mathcal{S}$, $Y \in \mathcal{Y}$, and $T \in \mathcal{T}$ be random variables. Then,*

1. *If the Markov chain $S \leftrightarrow X \rightarrow Y$ holds and the distributions of X and S are fixed, then $I(X; Y)$, $I(S; Y)$, and $I(X; Y|S)$ are convex functions with respect to the density $p_{Y|X}$.*
2. *If, additionally, the Markov chain $T \leftrightarrow X \rightarrow Y$ holds and the distributions of X , S , and T are fixed, then $I(X; Y|S, T)$ and $I(T; Y|S)$ are also convex functions with respect to the density $p_{Y|X}$.*

Proof. We start the proof leveraging (Cover and Thomas 2006, Theorem 2.7.4), which, in our setting, tells us that:

- $I(X; Y)$ is a convex function of $p_{Y|X}$ if p_X is fixed.
- $I(S; Y)$ is a convex function of $p_{Y|S}$ if p_S is fixed.

- $I(X; Y|S)$ is a convex function of $p_{Y|(X,S)}$ if $p_{X|S}$ is fixed.
- $I(X; Y|S, T)$ is a convex function of $p_{Y|(X,S,T)}$ if $p_{X|(S,T)}$ is fixed.
- $I(T; Y|S)$ is a convex function of $p_{Y|(S,T)}$ if $p_{T|S}$ is fixed.

Then, since $p_{Y|S} = \mathbb{E}_{p_{X|S}}[p_{Y|X}]$, $p_{Y|(X,S)} = \left(\frac{p_{X|S}}{p_X}\right) p_{Y|X}$, $p_{Y|(X,S,T)} = \left(\frac{p_{X|(S,T)}}{p_X}\right) p_{Y|X}$, and $p_{Y|(S,T)} = \mathbb{E}_{p_{X|(S,T)}}[p_{Y|X}]$ are non-negative weighted sums as defined in (Boyd, Boyd, and Vandenberghe 2004, 2.2.1), they preserve convexity. Hence, $I(S; Y)$, $I(X; Y|S)$, $I(X; Y|S, T)$, and $I(T; Y|S)$ are convex functions of $p_{Y|X}$, if p_S , $p_{X|S}$, $p_{X|(S,T)}$, and $p_{T|S}$ are fixed, respectively. \square

Proposition 4. *Let us consider that the distributions of S and X are fixed and that the conditional distribution $P_{Y|X}$ has a density $p_{Y|X}$. Then, the CPF optimization problem is not convex.*

Proof. From Lemma 1 we know that $I(S; Y)$ and $I(X; Y|S)$ are convex functions with respect to $p_{Y|X}$ for fixed p_S and $p_{X|S}$. Hence, the constraint $I(X; Y|S) \geq r$ is concave. \square

Proposition 5. *Let us consider that the distributions of S , T , and X are fixed and that the conditional distribution $P_{Y|X}$ has a density $p_{Y|X}$. Then, the CFB optimization problem is not convex.*

Proof. From Lemma 1 we know that $I(S; Y)$, $I(X; Y|S, T)$, and $I(T; Y|S)$ are convex functions with respect to $p_{Y|X}$ for fixed p_S , $p_{X|(S,T)}$, and $p_{T|S}$. Hence, the constraint $I(T; Y|S) \geq r$ is concave. \square

D Details of the experiments

In this section of the appendix, we include an additional experiment on the COMPAS dataset (Dieterich, Mendoza, and Brennan 2016) and describe the details of the experiments performed to validate the approach proposed in this paper. The code is at <https://github.com/burklight/VariationalPrivacyFairness>.

D.1 Results on the COMPAS dataset

COMPAS dataset. The ProPublica COMPAS dataset (Dieterich, Mendoza, and Brennan 2016)² contains 6, 172 samples of different attributes of criminal defendants in order to classify if they will recidivate within two years or not. These attributes include *gender*, *age*, or *race*. In both tasks, we followed the experimental set-up from Zhao et al. (2020) and considered S to be a binary variable stating if the defendant is African American and X to be the rest of attributes. For the fairness task, we considered T to be the binary variable stating if the defendant recidivated or not. Since this dataset was not previously divided between training and test set, we randomly splitted the dataset with 70% of the samples (4, 320) for training and the rest (1, 852) for testing.

²Available in the Kaggle website.

Table 3: Fairness metrics with different methods on the COMPAS dataset. Displayed as: Logistic regression / Random forest. The best hyperparameters for the other methods have been selected, as shown in the following section. These models are compared to our model with most similar results.

Methods	Accuracy (T)	Accuracy (S)	Discrimination	Error gap	EO gap
LFR (Zemel et al. 2013)	0.64 / 0.67	0.51 / 0.99	0.14 / 0.21	0.07 / 0.03	0.11 / 0.19
Ours ($\beta = 34.8$)	0.63 / 0.58	0.59 / 0.52	0.16 / 0.10	0.06 / 0.04	0.13 / 0.08
FFVAE (Creager et al. 2019, $\alpha = 200$)	0.54 / 0.51	0.50 / 0.50	0.00 / 0.01	0.12 / 0.05	0.00 / 0.04
CFAIR (Zhao et al. 2020, $\lambda = 10$) ³	-	-	0.04	0.00	0.02
Ours ($\beta = 7.76$)	0.54 / 0.52	0.52 / 0.49	0.00 / 0.02	0.14 / 0.04	0.00 / 0.03

Similarly to the previous experiments, the proposed approach controls the trade-off between private and informative representations and between fair and accurate representations. In Figure 7 we see how the trade-off between the compression level $I(X; Y)$ and the informativeness of the representations independent of the private data $I(X; Y|S)$ and between the compression level $I(X; Y)$ and the predictability of the representations without the sensitive data $I(X; Y|S)$ is controlled by the private and the fair representations, respectively. Moreover, we can also see how the amount of information the representations keep about the private or the sensitive data is commanded by the Lagrange multipliers γ and β .

Compared with other variational approaches to the PF (Nan and Tao 2020, PPVAE) and (Louizos et al. 2016, VFAE), as happened with the Adult dataset, the proposed approach controlled better the information the representations Y contained about the sensitive attribute S . In particular, the PPVAE contained between 0.63 and 1 bit of information about S for $\eta^{-1} \in [1, 50]$, and the VFAE contained between 0.68 and 1 bit for $\delta \in [N_{\text{batch}}, 1000N_{\text{batch}}]$. Note that 1 bit is the maximum information that Y can contain about S , since $H(S) = 1$ in this scenario. With respect to membership attacks, our method was a slightly weaker to linear attackers than the PPVAE and the VFAE, allowing an accuracy in the range $[0.54, 0.60]$, compared to their respective ranges of $[0.46, 0.62]$ and $[0.45, 0.59]$. That is, considering the prior probability of 0.51, the best parameter of our method conceded the attacker a 3% accuracy that the other methods did not allow. However, once the attacker employed more sophisticated attacks, such as a random forest, our method maintained a range of $[0.52, 0.56]$, while the PPVAE and the VFAE allowed almost a perfect recovery of the group membership, with respective accuracy ranges between 0.96 and 0.99 and between 0.96 and 1.0, as was suggested by the amount of bits of information their representations contained about S . As before, this behavior can be explained due to the Markov chain violation of the encoder densities $p_{Y|(S, X, \theta)}$ of these approaches.

Furthermore, the Lagrange multiplier β also allows us to control the behavior of the accuracy, the error gap, and the discrimination for the COMPAS dataset (Figures 8a, 8d,

and 8b). Moreover, in this scenario, as shown in Figures 8c and 8e, an increase of β also increased the equalized odds level and the accuracy on S of adversarial classifiers (even though they remained below their values obtained with the original data X for all the β tested). These results on the equalized odds, even though not generalizable since we have the counter-example of the Adult dataset, indicate that in some situations this quantity can be controlled with our approach. More specifically, we believe this happens when we can guarantee that $I(S; Y; T)$ is non-negative as explained in Remark 5.

Finally, we also observe, as for the Adult dataset, how the proposed method’s representations are more robust against non-linear adversaries than the representations obtained with the baseline from Zemel et al. (2013, LFR) (see Table 3). Moreover, the method performs similarly as state-of-the-art methods based on adversarial learning (Zhao et al. 2020, CFAIR) and variational inference (Creager et al. 2019, FFVAE), as shown in Table 3.

D.2 Experimental details

Encoders. In all the experiments performed, we modeled the encoding density as an isotropic Gaussian distribution, i.e., $p_{Y|(X, \theta)} = \mathcal{N}(Y; \mu_{\text{enc}}(X; \theta), \sigma_{\theta}^2 I_2)$, so that $Y = \mu_{\text{enc}}(X; \theta) + \sigma_{\theta} E$, where $E \sim \mathcal{N}(0, I_2)$, μ_{enc} is a neural network, σ_{θ} is also optimized via gradient descent but is not calculated with X as an input, and where the representations have 2 dimensions. The neural networks in each experiment were:

- For the Adult dataset, μ_{enc} was a multi-layer perceptron with a single hidden layer with 100 units and ReLU activations.
- For the Colored MNIST dataset, μ_{enc} was the convolutional neural network CNN-enc-1 for both the privacy and fairness experiments, and the convolutional neural network CNN-enc-2 for the example from Figure 5. Both architectures are described in Table 4.
- For the COMPAS dataset, μ_{enc} was a multi-layer perceptron with a single hidden layer with 100 units and ReLU activations.

Moreover, the marginal density of the representations was modeled as an isotropic Gaussian of unit variance and zero mean; i.e., $q_{Y|\theta} = \mathcal{N}(Y; 0, I_2)$.

³Results extracted from the original paper’s Figure 2. The fairness metrics were computed on the output of the discriminator network, not on an independent logistic regression or random forest.

Table 4: Convolutional neural network architectures employed for the Colored MNIST dataset. The network modules are the following: `Conv2D(cin, cout, ksize, stride, pin, pout)` and `ConvTrans2D(cin, cout, ksize, stride, pin, pout)` represent, respectively, a 2D convolution and transposed convolution, where `cin` is the number of input channels, `cout` is the number of output channels, `ksize` is the size of the filters, `stride` is the stride of the convolution, `pin` is the input padding of the convolution, and `pout` is the output padding of the convolution; `MaxPool2D(ksize, stride, pin)` represents a max-pooling layer, where the variables mean the same than for the convolutional layers; `Linear(nu)` represents a linear layer, where `nu` are the output units; and `BatchNorm`, `ReLU6`, `Flatten`, `Unflatten`, and `Sigmoid` represent a batch normalization, ReLU6, flatten, unflatten and Sigmoid layers, respectively.

Name	Architecture
CNN-enc-1	Conv2D(3, 5, 5, 2, 1, 0) - BatchNorm - ReLU6 - Conv2D(5, 50, 5, 2, 0, 0) - BatchNorm - ReLU6 - Flatten - Linear(100) - BatchNorm - ReLU - Linear(2)
CNN-enc-2	Conv2D(3, 5, 5, 0, 2, 0) - BatchNorm - ReLU6 - Conv2D(3, 5, 5, 0, 2, 0) - BatchNorm - ReLU6 - Conv2D(3, 5, 5, 0, 2, 0)
CNN-dec-1	Linear(100) - BatchNorm - ReLU6 - Linear(1250) - Unflatten - BatchNorm - ReLU - ConvTrans2D(50, 5, 5, 2, 0, 0) - BatchNorm - ReLU - ConvTrans2D(5, 3, 5, 2, 1, 1) - Sigmoid
CNN-dec-2	Conv2D(3, 5, 5, 0, 2) - BatchNorm - ReLU6 - Conv2D(5, 50, 5, 0, 2, 0) - BatchNorm - ReLU6 - Conv2D(5, 50, 5, 0, 2, 0) - BatchNorm - ReLU6 - Conv2D(5, 50, 5, 0, 2, 0) - Sigmoid
CNN-mine	Conv2D(3, 5, 5, 1, 1, 0) - MaxPool2D(5, 2, 2) - ReLU6 - Conv2D(5, 50, 5, 1, 0, 0) - MaxPool2D(5, 2, 2) - ReLU6 - Flatten - Linear(100) - ReLU6 - Linear(50) - ReLU6 - Linear(1)

Decoders. In all the experiments performed for the fairness problem, the target task variable T was binary. Hence, we modeled the inference density with a Bernoulli distribution⁴; i.e., $q_{T|(S, X, \phi)} = \text{Bernoulli}(T; \rho_{\text{dec}}(S, Y; \phi))$, where ρ_{dec} is a neural network with a Sigmoid activation function in the output. In the privacy problem, if X was a collection of random variables (X_1, X_2, \dots, X_C) , the generative density was modeled as the product of C categorical and isotropic Gaussians, depending if the variables were discrete or continuous. That is, $q_{X|(S, Y, \phi)} = \prod_{j=1}^C \text{Cat}(X_j; \rho_{\text{dec}, j}(S, Y; \phi))^{\mathbb{I}[X_j=\text{Discrete}]}$ $\mathcal{N}(X_j; \mu_{\text{dec}, j}(S, Y; \phi), \sigma_{\phi, j}^2)^{\mathbb{I}[X_j=\text{Continuous}]}$, where the continuous random variables are 1-dimensional. In practice, the densities were parametrized with a neural network with $K = \sum_{j=1}^C K_j^{\mathbb{I}[X_j=\text{Discrete}]} 1^{\mathbb{I}[X_j=\text{Continuous}]}$ output neurons, where K_j are the number of classes of the categorical variable X_j and each group of output neurons defines each multiplying density; either as the logits of the K_j classes or the parameter (mean) of the Gaussian (the variances were also optimized via gradient descent but were not calculated with S nor Y as an input). If X was an image, the generative density was modeled as a product of $3C$ Bernoulli densities, where C is the number of pixels of the image and the 3 comes from the RGB channels. The neural networks in each experiment were:

- For the Adult dataset, the decoding neural network was a multi-layer perceptron with a single hidden layer with

⁴Note that the Bernoulli distribution is a categorical distribution with two possible outcomes.

100 units and ReLU activations. For the fairness task, the output was 1-dimensional with a Sigmoid activation function. For the privacy task, the output was 121-dimensional. The input of the network was a concatenation of Y and S .

- For the Colored MNIST dataset and the fairness task, the decoding neural network was also a multi-layer perceptron with a single hidden layer with 100 units, ReLU activations, and a 1-dimensional output with a Sigmoid activation function. For the privacy task, the decoding neural network was the CNN-dec-1 for the normal experiments and the CNN-dec-2 for the example of Figure 5. The input linear layers took as an input a concatenation of Y and S and in the convolutional layers S was introduced as a bias.
- For the COMPAS dataset, the decoding neural network also was a multi-layer perceptron with a single hidden layer with 100 units and ReLU activations. For the fairness task, the output was 1-dimensional with a Sigmoid activation function. For the privacy task, the output was 19-dimensional. The input of the network was a concatenation of Y and S .

Hyperparameters and random seed. The hyperparameters employed in the experiments to train the encoder and decoder networks are displayed in Table 5, and the optimization algorithm used was Adam (Kingma and Ba 2014). All random seeds were set to 2020.

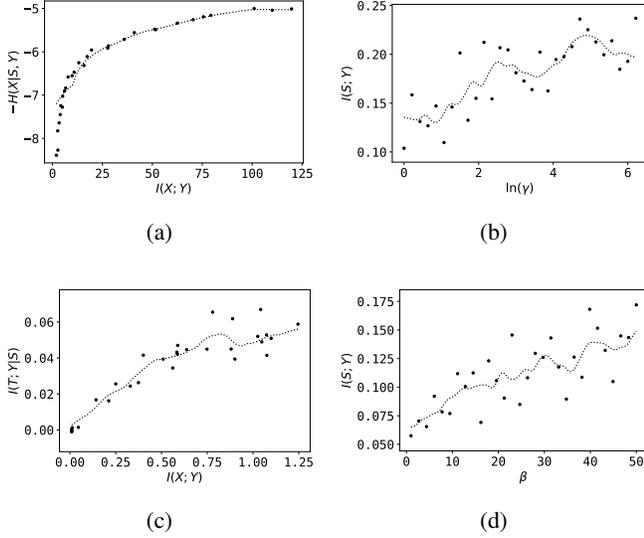


Figure 7: Trade-off between (a) the private representations compression $I(X; Y)$ and the non-private information retained $I(X; Y|S)$ and (b) the Lagrange multiplier $\gamma \in [1, 500]$ and the private information $I(S; Y)$ kept by the representations. Since $I(X; Y|S) = H(X|S) - H(X|S, Y)$ and $H(X|S)$ does not depend on Y , the reported quantity is $-H(X|S, Y)$. Moreover, trade-off between (c) the fair representations compression $I(X; Y)$ and the non-sensitive information retained about the task $I(T; Y|S)$ and (d) the Lagrange multiplier $\beta \in [1, 50]$ and the sensitive information kept by the representations. All quantities are obtained for the COMPAS dataset. The dots are the computed empirical values and the lines are the moving average of the 1D linear interpolations of such points.

Hardware and software. All experiments were run with PyTorch (Paszke et al. 2019), NumPy (Harris et al. 2020), and scikit-learn (Pedregosa et al. 2011) on a Nvidia Tesla P100 PCIE GPU of 16Gb of RAM.

Preprocessing. The input data X for the Adult and the COMPAS dataset was normalized to have 0 mean and unit variance. The input data for the Colored MNIST dataset was scaled to the range $[0, 1]$.

Information measures. The mutual information $I(X; Y)$ and the conditional entropy $I(X; Y|S)$ and $I(T; Y|S)$ were calculated with the bounds from (7), (8), and (9), respectively. Since $H(X|S)$ was not directly obtainable, $-H(X|S, Y)$ was calculated and displayed instead. The mutual information $I(S; Y)$ was calculated using the mutual information neural estimator (MINE) with a moving average bias corrector with an exponential rate of 0.1 (Belghazi et al. 2018); the resulting information was averaged over the last 100 iterations. The neural networks employed were a 2-hidden layer multi-layer perceptron with 100 ReLU6 activation functions for all the datasets and tasks, except

from the example on the Colored MNIST dataset, where the CNN-mine from Table 4 was used. In all tasks the input was a concatenation of S and Y , except from the example on the Colored MNIST dataset, where in all convolutional layers the private data S was added as a bias and in all linear layers S was concatenated to the input. The hyperparameters used to train the networks are displayed in Table 6.

Group fairness and utility indicators. The accuracy on T and S , the discrimination, and the error and equalized odds gaps were calculated using both the input data X and the generated representations Y . They were calculated with a Logistic regression (LR) classifier and a random forest (RF) classifier with the default settings from scikit-learn (Pedregosa et al. 2011). The prior displayed on the accuracy on T and S figures is the accuracy of a classifier that only infers the majority class of T and S , respectively, from the training dataset.

Comparison with PPVAE (Nan and Tao 2020). We implemented the algorithm as described in the original paper. We used the same neural network architecture (i.e., multi-layer perceptron with a single hidden layer with 100 units and ReLU activations) and training hyperparameters than in our method in order to provide a fair comparison. The original method was not prepared to handle other data that was not continuous, so we expanded the method assuming categorical, and Bernoulli output distributions for the non-continuous data. We studied 30 linearly equispaced values of the hyperparameter η^{-1} from (12) ranging from 1 to 50.

Comparison with VFAE (Louizos et al. 2016). We implemented the algorithm as described in the original paper. We used the same neural network architecture (i.e., multi-layer perceptron with a single hidden layer with 100 units and ReLU activations) and training hyperparameters than in our method in order to provide a fair comparison. We studied 30 linearly equispaced values of the hyperparameter δ multiplying the MMD term ranging from N_{batch} to $N_{\text{batch}}/1000$. We calculated the MMD using random kitchen sinks (Rahimi and Recht 2009) with $D = 500$ and $\gamma = 1$ as in the original paper.

Comparison with LFR (Zemel et al. 2013). We implemented the algorithm as described in the original paper. We used 10 prototypes ($K = 10$) and adjusted the hyperparameters A_x , A_y , and A_z so that the L-BFGS found a feasible solution in 150,000 iterations with a tolerance of 10^{-5} . We observed that different values of the hyperparameters (as noted by Zemel et al. (2013)) produced almost equivalent results, so we only report here the results for $A_x = 10^{-4}$, $A_y = 0.1$, and $A_z = 500$.

Comparison with FFVAE (Creager et al. 2019). We implemented the algorithm as described in the original paper. We used the same neural network architecture (i.e., multi-layer perceptron with a single hidden layer with 100 units

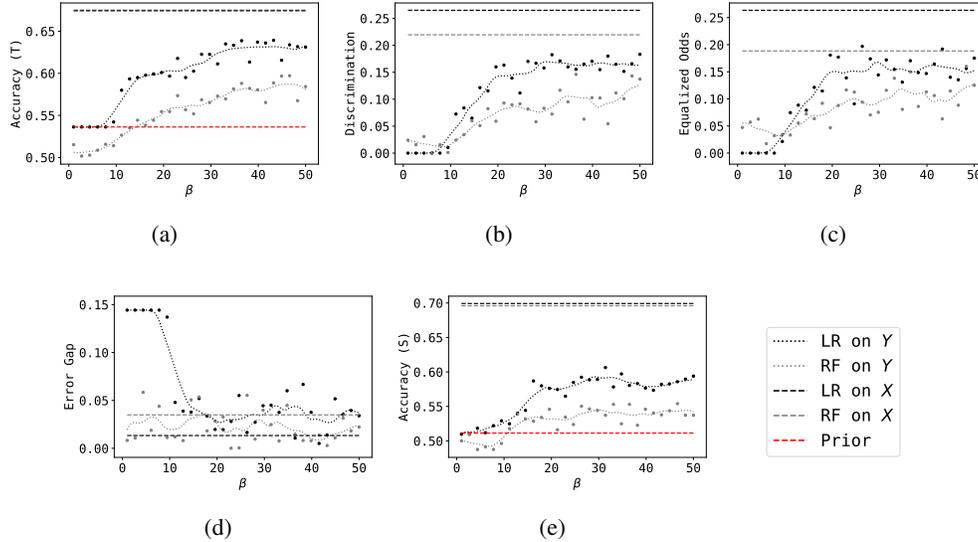


Figure 8: Behavior of (a) the accuracy on T , (b) the discrimination, (c) the equalized odds gap, (d) the error gap, and (e) the accuracy on S of a logistic regression (LR, in black) and a random forest (RF, in gray) of the fair representations (dots and dotted line) and the original data (dashed line) learned with $\beta \in [1, 50]$ on the COMPAS dataset. The dashed line in red is the accuracy of a prior-based classifier.

Table 5: Hyperparameters employed to optimize the encoder and decoder networks of the experiments.

Dataset (task)	Epochs	Learning rate	Lagrange multiplier (β or γ)	Batch size
Adult (fairness)	150	10^{-3}	1-50 (logarithmically spaced)	1024
Adult (privacy)	150	10^{-3}	1-50 (logarithmically spaced)	1024
Colored MNIST (fairness)	250	10^{-3}	1-50 (logarithmically spaced)	1024
Colored MNIST (privacy)	500	10^{-3}	1-50 (logarithmically spaced)	1024
Colored MNIST (example)	500	10^{-3}	1	2048
COMPAS (fairness)	150	10^{-4}	1-50 (linearly spaced)	64
COMPAS (privacy)	250	10^{-4}	1-500 (logarithmically spaced)	64

Table 6: Hyperparameters employed to optimize the MINE networks of the experiments.

Dataset (task)	Iterations	Learning rate	Batch size
Adult (fairness)	$5 \cdot 10^4$	10^{-3}	2048
Adult (privacy)	$5 \cdot 10^4$	10^{-3}	2048
Colored MNIST (fairness)	$5 \cdot 10^4$	10^{-3}	2048
Colored MNIST (privacy)	$5 \cdot 10^4$	10^{-3}	2048
COMPAS (fairness)	$5 \cdot 10^4$	10^{-3}	463
COMPAS (privacy)	$5 \cdot 10^4$	10^{-3}	463

and ReLU activations) and training hyperparameters than in our method in order to provide with a fair comparison. Since the sensitive variable has dimension 1, there was no need for an adversary discriminator and therefore the γ parameter was not explored. We performed experiments with different values of α ranging from 1 to 400 as in the original paper and we observed that the value of the hyperparameter did not modify much the results, as shown in Table 7. We selected $\alpha = 200$ for the comparisons since the results for that

α were the ones with the better trade-off between accuracy and fairness.

Comparison with CFAIR (Zhao et al. 2020). We implemented the algorithm as described in the original paper. For the experiments in the Adult dataset, we used the same neural network architecture (i.e., multi-layer perceptron with a single hidden layer with 100 units and ReLU activations)

Table 7: Fairness metrics with different values of α for the FFVAE. Displayed as: Logistic regression / Random forest.

Dataset	α	Accuracy (T)	Accuracy (S)	Discrimination	Error gap	EO gap
Adult	1	0.76 / 0.74	0.66 / 0.64	0.07 / 0.10	0.18 / 0.16	0.10 / 0.12
Adult	100	0.77 / 0.75	0.67 / 0.61	0.00 / 0.01	0.17 / 0.11	0.07 / 0.02
Adult	200	0.77 / 0.75	0.67 / 0.61	0.00 / 0.01	0.17 / 0.12	0.04 / 0.04
Adult	300	0.78 / 0.75	0.67 / 0.62	0.01 / 0.01	0.16 / 0.12	0.06 / 0.03
Adult	400	0.78 / 0.75	0.67 / 0.61	0.01 / 0.01	0.16 / 0.12	0.05 / 0.05
COMPAS	1	0.54 / 0.50	0.50 / 0.50	0.00 / 0.03	0.12 / 0.04	0.00 / 0.05
COMPAS	100	0.54 / 0.49	0.52 / 0.50	0.00 / 0.02	0.12 / 0.05	0.00 / 0.05
COMPAS	200	0.54 / 0.51	0.50 / 0.50	0.00 / 0.01	0.12 / 0.05	0.00 / 0.04
COMPAS	300	0.54 / 0.52	0.52 / 0.49	0.00 / 0.05	0.12 / 0.01	0.00 / 0.06
COMPAS	400	0.54 / 0.50	0.52 / 0.50	0.00 / 0.03	0.12 / 0.05	0.00 / 0.06

Table 8: Fairness metrics with different values of λ for the CFAIR. Displayed as: Logistic regression / Random forest.

Dataset	λ	Accuracy (T)	Accuracy (S)	Discrimination	Error gap	EO gap
Adult	0.1	0.78 / 0.74	0.68 / 0.67	0.03 / 0.03	0.14 / 0.12	0.01 / 0.00
Adult	1	0.77 / 0.71	0.68 / 0.63	0.03 / 0.04	0.17 / 0.09	0.17 / 0.11
Adult	10	0.77 / 0.70	0.67 / 0.64	0.00 / 0.03	0.17 / 0.10	0.04 / 0.04
Adult	100	0.77 / 0.71	0.67 / 0.63	0.05 / 0.03	0.17 / 0.09	0.22 / 0.08
Adult	1000	0.77 / 0.71	0.69 / 0.65	0.02 / 0.01	0.17 / 0.12	0.02 / 0.04

than in our method for the encoder, decoder, and the adversarial decoders, which are equipped with a gradient reversal layer (Ganin et al. 2016). Also, we employed the same training hyperparameters to ensure a fair comparison between the two methods. We performed experiments with different values of λ ranging from 0.1 to 1000 as in the original paper. However, for the experiments in the COMPAS dataset, we could not obtain good results with our architecture and hyperparameters nor could we replicate their results with their architecture and hyperparameters. Hence, for this dataset, we report here the results displayed in the original paper.

E Group fairness and utility indicators

In this section of the appendix, we define and put into perspective a series of metrics, employed in this article, that indicate the predicting and group fairness quality of a classifier.

Notation Let $X \in \mathcal{X}$, $S \in \mathcal{S}$, and $T \in \mathcal{T}$ be random variables denoting the input data, the sensitive data, and the target task data, respectively. Let also $\mathcal{X} \subseteq \mathbb{R}^{d_x}$, $\mathcal{S} = \{0, 1\}$, and $\mathcal{T} = \{0, 1\}$. Let $w : \mathcal{X} \rightarrow \mathcal{T}$ be a classifier; that is, $w \in \mathcal{W}$ is a function that receives as an input an instance of the input data $x \in \mathcal{X}$ and outputs an inference about the target task value $t \in \mathcal{T}$ for that input data. Let us also consider the setting where we have a dataset that contains N samples of the random variables, i.e., $D = \{(x^{(i)}, s^{(i)}, t^{(i)})\}_{i=1}^N$. Finally, let \hat{P} denote the empirical probability distribution on the dataset D , $\hat{P}_{S=\sigma}$ the empirical probability distribution on the subset of the dataset D where $s^{(i)} = \sigma$, i.e., $\{(x, s, t) \in D : s = \sigma\}$,

and $\hat{P}_{(S=\sigma, T=\tau)}$ the empirical probability distribution on the subset of the dataset D where $s^{(i)} = \sigma$ and $t^{(i)} = \tau$, i.e., $\{(x, s, t) \in D : s = \sigma \text{ and } t = \tau\}$.

A common metric to evaluate the performance (utility) of a classifier w on a dataset is its *accuracy*, which measures the fraction of correct classifications of w on such a dataset.

Definition 1. The accuracy of a classifier w on a dataset D is

$$\text{Accuracy}(w, D) = \hat{P}(w(X) = T). \quad (30)$$

An ideally fair classifier w would maintain *demographic parity* (or *statistical parity*) and *accuracy parity*, which, respectively, mean that $w(X) \perp S$ (or, equivalently if w is deterministic, that $\hat{P}_{S=0}(w(X) = 1) = \hat{P}_{S=1}(w(X) = 1)$) and that $\hat{P}_{S=0}(w(X) \neq T) = \hat{P}_{S=1}(w(X) \neq T)$ (Zhao et al. 2020). In other words, if a classifier has demographic parity, it means that it gives a positive outcome with equal rate to the members of $S = 0$ and $S = 1$. However, demographic parity might damage the desired utility of the classifier (Hardt, Price, and Srebro 2016), (Zhao and Gordon 2019, Corollary 3.3). Accuracy parity, on the contrary, allows the existence of perfect classifiers (Zhao et al. 2020). The metrics that assess the deviation of a classifier from demographic and accuracy parities are the *discrimination* or *demographic parity gap* (Zemel et al. 2013; Zhao et al. 2020) and the *error gap* (Zhao et al. 2020).

Definition 2. The discrimination or demographic parity gap of a classifier w to the sensitive variable S on a dataset D is

$$\text{Discrimination}(w, D) = \left| \hat{P}_{S=0}(w(X) = 1) - \hat{P}_{S=1}(w(X) = 1) \right|. \quad (31)$$

Definition 3. The error gap of a classifier w with respect to the sensitive variable S on a dataset D is

$$\text{Error gap}(w, D) = \left| \hat{P}_{S=0}(w(X) \neq T) - \hat{P}_{S=1}(w(X) \neq T) \right|. \quad (32)$$

Another advanced notion of fairness is that of *equalized odds* or *positive rate parity*, which means that $\hat{P}_{(S=0, T=\tau)}(w(X) = 1) = \hat{P}_{(S=1, T=\tau)}(w(X) = 1)$, for all $\tau \in \{0, 1\}$ or, equivalently, that $w(X) \perp S \mid T$ (Hardt, Price, and Srebro 2016). This notion of fairness requires that the true positive and false positive rates of the groups $S = 0$ and $S = 1$ are equal. The metric that assesses the deviation of a classifier from equalized odds is the *equalized odds gap* (Zhao et al. 2020).

Definition 4. The equalized odds gap of a classifier w with respect to the sensitive variable S on a dataset D is

$$\text{Equalized odds gap}(w, D) = \max_{\tau \in \{0, 1\}} \left| \hat{P}_{(S=0, T=\tau)}(w(X) = 1) - \hat{P}_{(S=1, T=\tau)}(w(X) = 1) \right|. \quad (33)$$

Remark 3. In the particular case of learning fair representations, the classifier $w : \mathcal{X} \rightarrow \mathcal{T}$ consists of two stages: an encoder $w_{\text{enc}} : \mathcal{X} \rightarrow \mathcal{Y}$ and a decoder $w_{\text{dec}} : \mathcal{Y} \rightarrow \mathcal{T}$, where the intermediate variable $Y = w_{\text{enc}}(X)$ is the fair representation of the data. Therefore:

1. Minimizing $I(S; Y)$ encourages demographic parity, since

$$I(S; Y) = 0 \iff Y \perp S \implies w(X) \perp S. \quad (34)$$

2. Minimizing $I(S; Y|T)$ encourages equalized odds, since

$$I(S; Y|T) = 0 \iff Y \perp S \mid T \implies w(X) \perp S \mid T. \quad (35)$$

Remark 4. Based on Remark 3, we note that the variational approach to the CFB and the CPF for generating private and/or fair representations encourages demographic parity, since the minimization of the Lagrangians of such problems, \mathcal{L}_{CFB} and \mathcal{L}_{CPF} , indeed minimizes $I(S; Y)$.

Remark 5. Contrary to Remark 4 concerning the minimization of the demographic parity gap, we cannot say that the variational approach to the CFB and the CPF minimizes the equalized odds gap.

Even though $I(S; Y) = I(S; Y|T) + I(S; Y; T)$, since $I(S; Y; T)$ can be negative (Yeung 1991), then $I(S; Y)$ is not necessarily greater than $I(S; Y|T)$ and thus there is no guarantee that minimizing $I(S; Y)$ will minimize $I(S; Y|T)$ as well.

Therefore, the minimization of \mathcal{L}_{CFB} and \mathcal{L}_{CPF} , which minimizes $I(S; Y)$, also minimizes the equalized odds gap when $I(S; Y; T) \geq 0$ and therefore $I(S; Y) \geq I(S; Y|T)$. That is, the CFB and the CPF minimize the equalized odds gap when there is no synergy between X and Y to learn about S ; i.e., $I(S; Y) + I(S; X) \geq I(S; (X, Y))$.

Continuing with the reflection on Remarks 3 and 5, a constrained optimization formulation *a la* CPF that leads to a minimization of the equalized odds gap is possible. Namely,

$$\arg \inf_{P_{Y|X}} \{I(S; Y|T) + I(X; Y|S, T)\} \text{ s.t. } I(T; Y|S) \geq r, \quad (36)$$

which minimizes the dark and darker gray areas from Figure 1a, which correspond to the sensitive and irrelevant data, respectively, except the intersection between the sensitive data S , the representations Y , and the target T , which corresponds to $I(S; Y; T)$. In this formulation, it is ensured that the representations Y also maintain a certain level of the information r of the target that is not shared in the sensitive data $I(T; Y|S)$.

F Motivation of mutual information as utility and privacy/fairness metric

The main to choose mutual information (and conditional mutual information) as the measure of utility and privacy and/or fairness is the tractability of this metric and the fact that it allowed us to (i) draw connections between the privacy and fairness problems and (ii) derive an algorithm that could be easily incorporated to current approaches to representation learning.

Other than that, even though there are some caveats of using mutual information as a measure of privacy (see (Issa, Wagner, and Kamath 2019)) or fairness, this metric has several operational meanings. Namely:

- **Utility.** The conditional mutual information $I(X; Y|S)$ (or $I(T; Y|S)$) is a measure of the relevance of the representation Y to explain X (or T). This is in line with the information bottleneck (Tishby, Pereira, and Bialek 2000; Alemi et al. 2016; Kolchinsky, Tracey, and Wolpert 2019) and other common representation learning algorithms (Hjelm et al. 2018; Makhdoumi et al. 2014). An intuition would be that if we want to keep the average distortion smaller than a certain quantity, and we consider the distortion to be the log-loss, then we want that the (conditional) mutual information is greater than a, different, certain quantity (see e.g. (Makhdoumi et al. 2014, Section III-B)).
- **Privacy.** The mutual information $I(S; Y)$ is the average cost gain by an adversary with the self-information or log-loss cost function (Makhdoumi et al. 2014, Lemma 1). This has also been used in other works such as (Chatzikokolakis, Chothia, and Guha 2010; Zhu and Bet-tati 2005). Moreover, an upper bound on mutual information limits both the Bayesian and minimax risks that can be achieved in any inference based on the data; see e.g. (Wainwright 2019, Chapter 15.3 on Fano’s method).
- **Fairness.** As explained in Remark 3 minimizing $I(S; Y)$ encourages demographic parity and minimizing $I(S; Y|T)$ encourages equalized odds.